J Nanopart Res (2012) 14:713
DOI 10.1007/s11051-011-0713-4

RESEARCH PAPER

Preparation and characterization of spinel $Li_4Ti_5O_{12}$ nanoparticles anode materials for lithium ion battery

Hongli Wu · Yudai Huang · Dianzeng Jia · Zaiping Guo · Ming Miao

Received: 11 May 2011 / Accepted: 28 December 2011 / Published online: 12 January 2012

Abstract Spinel $Li_4Ti_5O_{12}$ nanoparticles were prepared via a high-temperature solid-state reaction by adding the prepared cellulose to an aqueous dispersion of lithium salts and titanium dioxide. The precursors of $Li_4Ti_5O_{12}$ were characterized by thermogravimetry and differential scanning calorimetry. The obtained $Li_4Ti_5O_{12}$ nanoparticles were characterized using X-ray diffraction, transmission electron microscopy (TEM) and electrochemical measurements. The TEM revealed that the $Li_4Ti_5O_{12}$ prepared with cellulose is composed of nanoparticles with an average particle diameter of 20–30 nm. Galvanostatic battery testing showed that nano-sized $Li_4Ti_5O_{12}$ exhibit better electrochemical properties than submicro-sized $Li_4Ti_5O_{12}$ do especially at high current rates, which can deliver a reversible discharge capacity of 131 mAh g^{-1} at the rate of 10 C, whereas that of the submicro-sized sample decreases to 25 mAh g^{-1} at the same rate (10 C). Its reversible capacity is maintained at $\sim$172.2 mAh g^{-1} with the voltage range 1.0–3.0 V (vs. Li) at the current rate of 0.5 C for over 80 cycles.

Keywords Spinel $Li_4Ti_5O_{12}$ nanoparticles · Cellulose · Anode material · Lithium ion battery · Energy storage

H. Wu · Y. Huang · D. Jia
Key Laboratory of Clean Energy Material and Technology of the Ministry of Education, Xinjiang University, Urumqi 830046, Xinjiang, People's Republic of China

H. Wu · Y. Huang · D. Jia
Key Laboratory of Advanced Functional Materials of the Autonomous Region, Xinjiang University, Urumqi 830046, Xinjiang, People's Republic of China

H. Wu · Y. Huang · D. Jia (✉)
Institute of Applied Chemistry, Xinjiang University, Urumqi 830046, Xinjiang, People's Republic of China
e-mail: jdz0991@gmail.com

Z. Guo
Institute for Superconducting and Electronic Materials, University of Wollongong, Wollongong, NSW 2522, Australia

M. Miao
Xinjiang Cancer Institute & Hospital, Urumqi, People's Republic of China

Introduction

It is well known that lithium ion batteries with high energy and power density have attracted much attention due to be extensively used for consumer electronic devices, portable power tools and vehicle electrifications (Kim et al. 2008). In the present commercial lithium ion batteries, graphite has been widely used as the lithium ion battery anode due to its even discharge–charge potential profile and low cost. Unfortunately, graphite has some disadvantages and cannot meet satisfactorily the performance requirements of some important applications, especially in the safety and rate performance (Qiao et al. 2008;

Ge et al. 2008; Shen et al. 2006; Wang et al. 2006). As a result, alternative anode materials have attracted much interest. One promising candidate is spinel $Li_4Ti_5O_{12}$, which has a theoretical capacity of 175 mAh g^{-1}, a flat discharge potential of 1.56 V versus Li/Li^+ and other advantages, such as low cost, environmental friendliness, excellent electrochemical properties and high safety. In addition, this spinel material, as a zero-strain insertion material, was proposed for anodes in lithium secondary batteries since there is no structural change during the insertion/extraction of lithium ions (Liu et al. 2009; Gao and Tang 2008; Gao et al. 2006). In recent years, spinel anode material $Li_4Ti_5O_{12}$ has been extensively and deeply studied as an attractive anode material for lithium ion batteries.

However, as an insulator, the low rate capacity of $Li_4Ti_5O_{12}$ resulting from poor electronic conductivity and its low tap density is the main impediment to commercialization. In fact, many new approaches have suggested solutions to improve the conductivity as follows (Jin et al. 2008; Gaberscek et al. 2007; Qi et al. 2009; Wang et al. 2006): (1) coating with an electron-conducting phase; (2) ionic substitution to enhance the electrochemical properties; and (3) particle size minimization while synthesizing the nano-sized particles as one of the most effective methods. Synthesizing the nano-sized $Li_4Ti_5O_{12}$ could heighten the electrochemical performance of electrode materials, because small particle size will not only obviously shorten Li^+ diffusion path and broaden the electrode/electrolyte contact surface, but also decrease the charge-transfer resistance of the electrodes (Jiang et al. 2006; Croce et al. 1998; Yi et al. 2010). However, it is very difficult to control the $Li_4Ti_5O_{12}$ sizes via an easy way of solid-state reaction at high temperature.

We report a facile method with simple raw materials to synthesize $Li_4Ti_5O_{12}$ nanoparticles. The rate capability of the nano-sized $Li_4Ti_5O_{12}$ has been improved significantly compared to that of submicro-sized $Li_4Ti_5O_{12}$ prepared by the same method. Although Yuan et al. (2009a, b, 2010) have indeed used cellulose during the preparation process, the obtained particle size is 0.2–0.8 μm and its discharge capacity is around 120 mAh g^{-1} at 10 C. In our paper, the transmission electron microscopy (TEM) image of the as-prepared $Li_4Ti_5O_{12}$ used cellulose shows that all the particles are nano-sized and well distributed; the particle diameter is in the range of 20–30 nm, and discharge capacity is about 130 mAh g^{-1} at the same current rate (10 C).

Experimental

Synthesis of cellulose

20 mL concentrated H_2SO_4 (98%) and 10 mL concentrated HNO_3 (68%) were mixed together and stirred, and then absorbent cotton was added and immersed in this mixture for 30 min. Thereafter, the product was washed with distilled water several times to remove other ions and the acid, and then dried at 60 °C for 12 h. The obtained cellulose was milled for further use (Shen et al. 2006).

$Li_4Ti_5O_{12}$ preparation

42 mmol $LiAc{\cdot}H_2O$, 50 mmol TiO_2 and the prepared cellulose (2 g) were put in deionized water and stirred for 6 h. Excess Li was added to compensate for lithium volatilization loss during the high temperature of synthesis (Qi et al. 2009; Huang et al. 2011). The mixture was dried at 100 °C to remove water and the solid precipitated product was obtained. Then the solid precipitated product was preheated at 300 °C for 2 h to produce powder, which was put into an agate mortar and ground with a pestle for 0.5 h to get a well-mixed powder, and then it was calcined in air at 800 °C for 10 h in a muffle furnace. The $Li_4Ti_5O_{12}$ nanoparticles were obtained. The submicro-sized $Li_4Ti_5O_{12}$ was synthesized as above but without adding cellulose.

Characterization

The thermal decomposition behavior of the $Li_4Ti_5O_{12}$ precursor powders was examined by means of thermogravimetry and differential scanning calorimetry (TG-DSC; STA449F3, NETZSCH, Germany) at a heating rate of 10 °C min^{-1}. Powder X-ray diffraction (XRD; MXP18AHF, MAC, Japan) using Cu Kα radiation ($\lambda = 1.54056$ Å) was used to identify the phase composition of the synthesized powders. The grain size and structure of the samples were observed using TEM (H-600, HITACHI, Japan) with an accelerating voltage of 100 kV. The electronic conductivity of the samples was measured by using 4-point probes

resistivity measurement system (RTS-9; PROBES, China). The surface areas of the samples were estimated by Brunauer-Emmett-Teller (BET; JW-BK, China).

Electrochemical measurements

The anodes were prepared by mixing 75 wt% $Li_4Ti_5O_{12}$ powders with 15 wt% acetylene black, and 10 wt% polyvinylidene fluoride (as binder) in *N*-methylpyrrolidone and with Cu foil as the current collector. Lithium foil was used as the counter electrode, and the separator was a Celgard 2400 microporous polyethylene membrane. The electrolyte was 1 M $LiPF_6$/EC + DEC (1:1, v/v). CR2032-type coin cells were assembled in an argon-filled glove box. Galvanostatic charge and discharge were controlled between 1.0 and 3.0 V on a cell test instrument (LAND CT2001, KINGNUO, China) at room temperature. The cyclic voltammetry was carried out on a CHI600B Electrochemical Workstation (CHI, 600B, CHENHUA, China) in the potential range of 1.0–3.0 V at a scan rate of 0.1 mV s^{-1}. Electrochemical impedance spectroscopy measurements were performed using an impedance system (IM6ex, ZAHNER ELEKTRIK, Germany). The spectrum was potentiostatically measured by applying an ac voltage of 5 mV over the frequency range from 0.01 Hz to 100 kHz.

Results and discussion

Figure 1 exhibits the result of simultaneous TG-DSC of the $Li_4Ti_5O_{12}$ precursors obtained by adding cellulose or not. Figure 1a exhibits the result of simultaneous TG-DSC of a mixture containing $LiAc{\cdot}H_2O$ and TiO_2. Two significant weight losses can be detected in Fig. 1a: the first one occurs between 60 and 260 °C ($\Delta m = 4.57\%$) and is associated with release of physically adsorbed water process; the second one ($\Delta m = 16.41\%$) occurs between 260 and 600 °C and can be related to release of the water of crystallization and thermal decomposition of the partial reactants. Figure 1b exhibits the result of simultaneous TG-DSC of a mixture containing $LiAc{\cdot}H_2O$, TiO_2 and the prepared cellulose. The TG curve of Fig. 1b presents two steps of weight loss. Release of an amount of physically absorbed water and cellulose occurs between 60 and 260 °C ($\Delta m = 19.62\%$), and because of loss of cellulose, there is more weight loss than that shown in Fig. 1a. A continuous weight

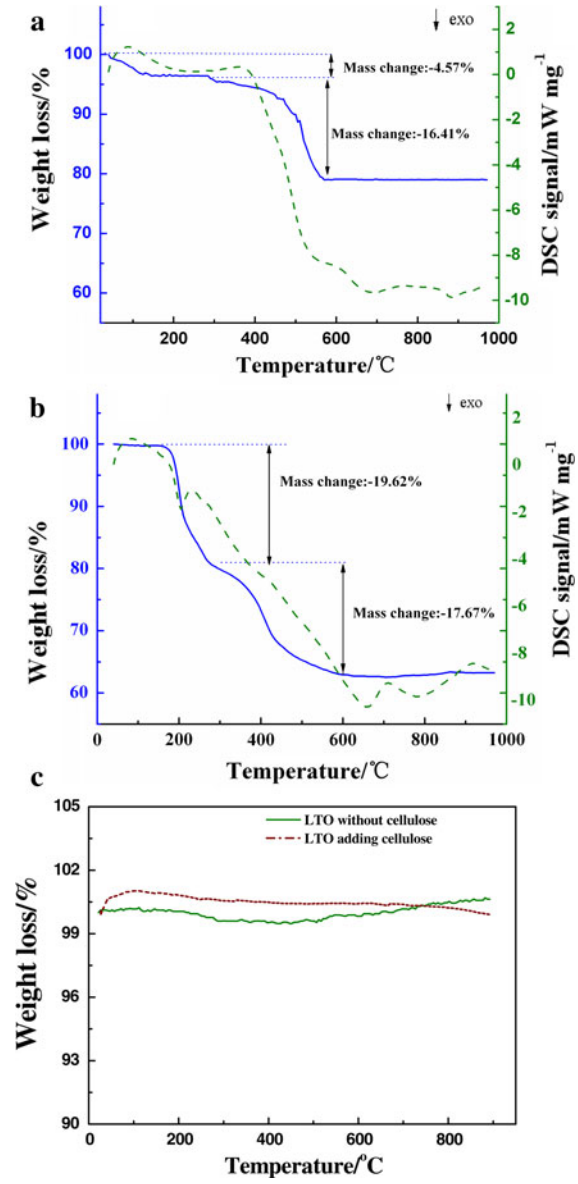

Fig. 1 TG-DSC analyses conducted on $Li_4Ti_5O_{12}$ precursors obtained by **a** without cellulose; **b** adding cellulose; **c** TG analyses about the synthesized $Li_4Ti_5O_{12}$ with/without cellulose in air to 900 °C

loss between 260 and 600 °C can be related to the release of the water of crystallization and thermal decomposition of the partial reactants. Judging from the difference of the weight loss between Fig. 1a and b, the decomposition of cellulose can be confirmed by the TG-DSC curves between 60 and 260 °C as shown in Fig. 1b. There is an obvious exothermic DSC peak at 650 °C, suggesting that the crystallization of

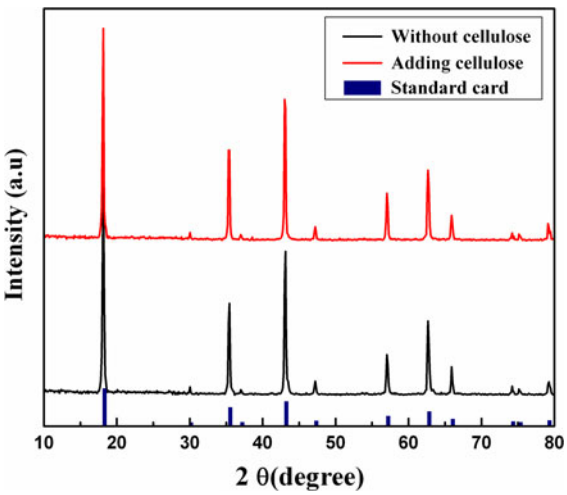

Fig. 2 The XRD patterns for $Li_4Ti_5O_{12}$ synthesized by adding cellulose or not

$Li_4Ti_5O_{12}$ forms above this temperature. Therefore, it is necessary to calcine the $Li_4Ti_5O_{12}$ precursor above 650 °C to obtain the crystallized phase (Shen et al. 2006; Wang et al. 2006). In this study, thermal conversion into $Li_4Ti_5O_{12}$ and subsequent crystalline growth was finished by preheating the precursor at 300 °C for 2 h to produce powder. The obtained powder was then calcined at 800 °C in air for 10 h. Figure 1c shows a small amount of weight loss of carbon in $Li_4Ti_5O_{12}$ synthesized with cellulose. The presence of carbon can improve the electrical conductivity of $Li_4Ti_5O_{12}$.

Figure 2 shows the XRD patterns for $Li_4Ti_5O_{12}$ synthesized by adding cellulose or not, which were collected using Cu Kα radiation ($\lambda = 1.54056$ Å). The diffraction patterns confirm that both the crystal structures are coincident with the spinel $Li_4Ti_5O_{12}$ standard in the Joint Committee on Powder Diffraction Standards database (JCPDS No. 49-0207). No impurity was detected from the XRD patterns of the samples, indicating that the two samples have the cubic spinel structure (Liu et al. 2009). From the XRD patterns, we can see that $Li_4Ti_5O_{12}$ were synthesized successfully by adding cellulose or not, and the added cellulose does not change the cubic structure of spinel $Li_4Ti_5O_{12}$.

TEM image of the synthesized $Li_4Ti_5O_{12}$ without adding cellulose reveals that the particles are mainly submicro-sized, and the particle shapes are not regular as shown in Fig. 3a. Figure 3b shows the TEM image of the $Li_4Ti_5O_{12}$ by adding cellulose, in which we can clearly see that all the particles are nano-sized, well-distributed and the particle diameter is in the range of 20–30 nm. Here cellulose works as an absorbing agent and a kind of dispersant, which could easily absorb metal ions so that the metal ions could be effectively distributed on the surface of cellulose. The aggregation of metal ions can be prevented (Shen et al. 2006). It is obvious that addition of cellulose avoids effectively the growing of crystal grain exceptionally to overcome the agglomeration of particles. The sample added cellulose can provide higher surface area and better electrical conductivity. In order to confirm this,

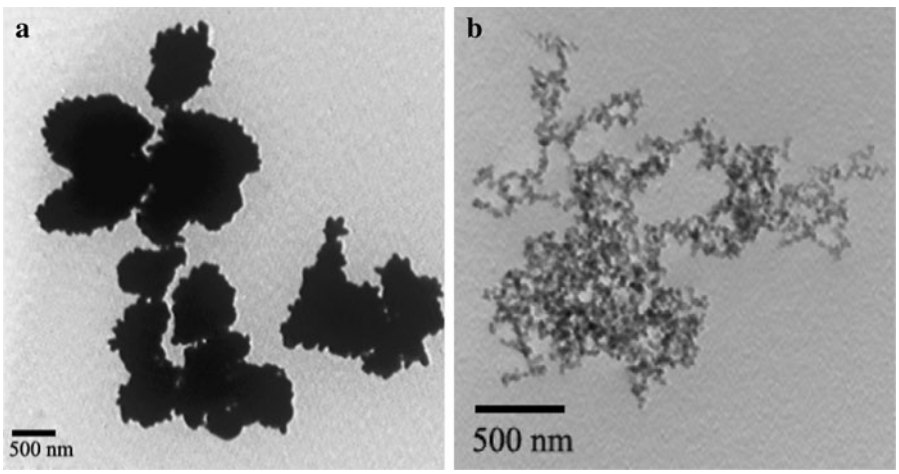

Fig. 3 TEM images of the samples: **a** $Li_4Ti_5O_{12}$ prepared without adding cellulose; **b** $Li_4Ti_5O_{12}$ prepared by adding cellulose

Table 1 Electrical conductivity and BET area of the samples

Samples	Electrical conductivity (S cm^{-1})	BET area (m^2 g^{-1})
$Li_4Ti_5O_{12}$ submicron particles	$<10^{-8}$	16.6
$Li_4Ti_5O_{12}$ nanoparticles	1.8×10^{-7}	48.9

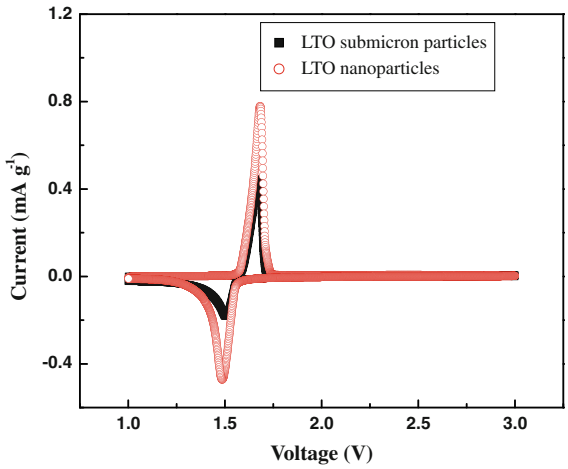

Fig. 4 Cyclic voltammograms of nano-sized $Li_4Ti_5O_{12}$ and submicro-sized $Li_4Ti_5O_{12}$

we have carefully tested the electrical conductivity and BET surface area for comparison with both of the samples as shown in Table 1. It can been seen clearly that the surface area of the sample prepared by adding cellulose is almost three times of that of the sample without adding cellulose, and the electrical conductivity of the sample prepared by adding cellulose is higher than that of the sample without adding cellulose. The results indicate that the $Li_4Ti_5O_{12}$ prepared with cellulose has ideal spinel structure, regular shape, narrow particle size distribution, higher surface area and electrical conductivity improved by residual carbon from calcining of cellulose.

Figure 4 shows the cyclic voltammograms (CVs) of nano-sized $Li_4Ti_5O_{12}$ and submicro-sized $Li_4Ti_5O_{12}$ in the potential range of 1.0–3.0 V at the scan rates of 0.1 mV s^{-1}. Each curve clearly demonstrates that there is one pair of redox peaks in the range of 1.0–3.0 V, which is in accordance with the typical CV characteristics of spinel $Li_4Ti_5O_{12}$. The redox peaks should be attributed to the oxidation and reduction of Ti^{3+}/Ti^{4+} accompanied along with Li^+ insertion/extraction in the materials (Wang et al. 2009; Yi et al.

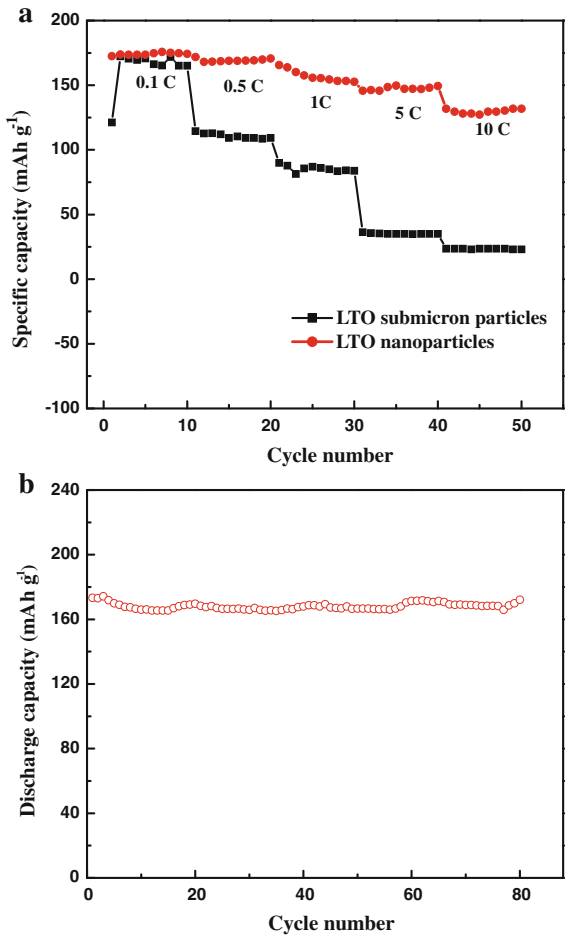

Fig. 5 **a** Rate performance of the nano-sized $Li_4Ti_5O_{12}$ and submicro-sized $Li_4Ti_5O_{12}$ at different current densities. **b** Graph of specific discharge capacity versus cycle number for $Li_4Ti_5O_{12}$ nanoparticles at the current density of 0.5 C

2009). However, compared with submicro-sized $Li_4Ti_5O_{12}$, the peak currents and integrated peak area of nano-sized $Li_4Ti_5O_{12}$ are much higher, indicating that nano-sized $Li_4Ti_5O_{12}$ have a higher capacity and reactivity. These confirm that the $Li_4Ti_5O_{12}$ nanoparticles have good reversibility and the nano-sized structure is very advantageous for the transportation of Li^+.

Figure 5a shows the rate performance of the nano-sized $Li_4Ti_5O_{12}$ and submicro-sized $Li_4Ti_5O_{12}$ at different current densities (0.1, 0.5, 1, 5 and 10 C). We have observed that nanostructured $Li_4Ti_5O_{12}$ has a much higher discharge capacity with increasing in current density. At the lowest current rate of 0.1 C (from cycles 1–10), both the samples have a specific

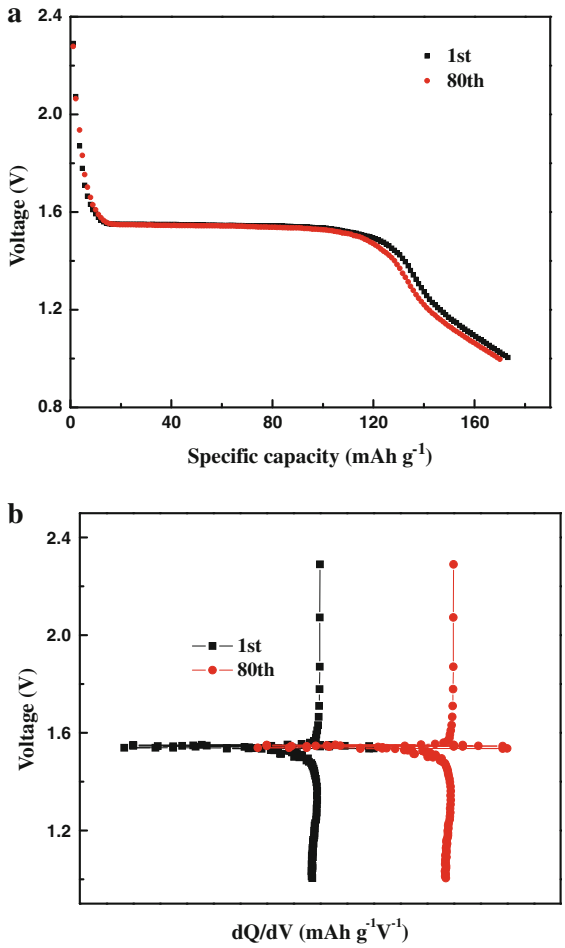

Fig. 6 **a** The 1st and the 80th discharge curves (0.5 C), and **b** the 1st and the 80th differential capacity (dQ/dV) versus voltage for $Li_4Ti_5O_{12}$ nanoparticles

discharge capacity around 173 mAh g^{-1}, which is close to the theoretical capacity, but with increasing current density from 0.5 to 10 C (from cycles 11–50), it leads to a large difference in performance, especially at 10 C; the specific discharge capacity of the nano-sized $Li_4Ti_5O_{12}$ remains almost 128 mAh g^{-1}, while that of the other sample decreases to 25 mAh g^{-1}. This improvement might be attributable to the high surface area and high electrical conductivity of the nanostructured materials (Liu et al. 2009). The data indicate that the large surface-to-volume ratio of nano-sized particle enhances the kinetics of the $Li_4Ti_5O_{12}$ electrodes. To evaluate the discharge capacity retention, the nano-sized $Li_4Ti_5O_{12}$ was performed 80 cycles at 0.5 C (Fig. 5b). The sample shows very good discharge capacity retention and the discharge capacity retention after 80 cycles is about 99.4%. The results come from the nano-sized active materials which can supply larger electrode/electrolyte contact area. Therefore, the nano-sized $Li_4Ti_5O_{12}$ material shows excellent discharge capacity retention through the reduction of particle size (Kim et al. 2008; Croce et al. 1998; Yi et al. 2010).

The electrochemical results are shown in terms of voltage versus discharge capacity (Fig. 6a) and voltage versus differential capacity (dQ/dV) (Fig. 6b) in the 1st and 80th discharge process at 0.5 C of nano-sized $Li_4Ti_5O_{12}$. The 1st and 80th discharge capacities were 173.3 and 172.2 mAh g^{-1}, respectively, with a voltage plateau at about 1.56 V versus Li/Li^+. From the 1st cycle to the 80th cycle, the capacity loss is about 0.6%, which illustrates that discharge capacity retention remains at 99.4% throughout the cycling process. The voltage versus dQ/dV curves clearly display a spike peak at about 1.56 V (Fig. 6b), which corresponds to a flat discharge plateau (Fig 6a). The voltage versus dQ/dV curve over 80 cycles is nearly the same as that of the 1st cycle, which can be inferred that $Li_4Ti_5O_{12}$ nanoparticles have better cycling behavior and stability.

The curves of Fig. 7 present typical Nyquist plots of the nano-sized $Li_4Ti_5O_{12}$ and submicro-sized $Li_4Ti_5O_{12}$. The plots are similar to each other in shape, with a semicircle line appearing in the high-frequency domain and a straight line in the low-frequency region. The depressed semicircle in the moderate frequency region is attributed to the charge-transfer process (Liu et al. 2009; NuLi et al. 2008). Compared with the results

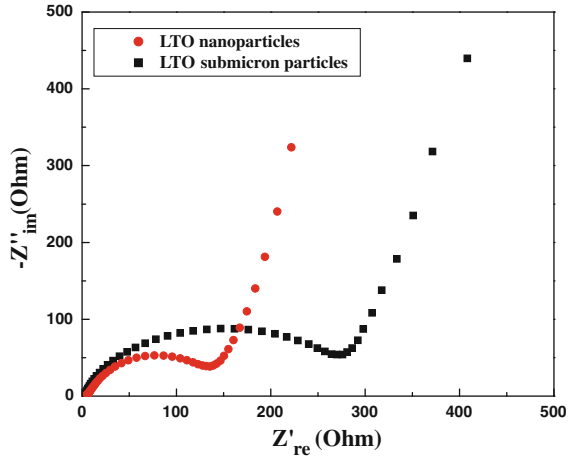

Fig. 7 Nyquist plots of the nano-sized $Li_4Ti_5O_{12}$ and submicro-sized $Li_4Ti_5O_{12}$

shown, it can be seen that the semicircle for the nano-sized sample is smaller. The charge-transfer resistance of the nano-sized $Li_4Ti_5O_{12}$ electrode is around 140 Ω, while that of submicro-sized $Li_4Ti_5O_{12}$ electrode is above 270 Ω. This indicates that the nano-sized particles decrease charge-transfer resistance (Maier 2007), which is in good agreement with the electrochemical test results above.

Conclusions

Nano-sized $Li_4Ti_5O_{12}$ was obtained by adding cellulose to TiO_2 and $LiAc{\cdot}H_2O$ by a high-temperature solid-state reaction. The added cellulose does not affect the spinel structure. Moreover, due to the fine particle size and large surface area, nano-sized $Li_4Ti_5O_{12}$ showed better electrochemical performance, with the good discharge capacity retention of 99.4% after the 80th cycle at 0.5 C and less inner resistance, higher reversibility and the discharge capacity of 131 mAh g^{-1} at 10 C, which is remarkably higher than that of the submicro-sized $Li_4Ti_5O_{12}$.

Acknowledgments This work was supported by the Natural Science Foundation of Xinjiang Province (No. 200821121), the National Natural Science Foundation of China (Nos. 21161021 and 21061013), the Technological People Service Corporation (No. 2009GJG40028), the Science and Technology Foundation of Urumqi (Nos. y08231006 and ZD8113007), the Science and Technology Foundation of Xinjiang University (No. BS100114), and the Program for Changjiang Scholars and Innovative Research Team in University of Ministry of Education of China (No. IRT1081).

References

Croce F, Appetecchi GB, Persi L, Scrosati B (1998) Nanocomposite polymer electrolytes for lithium batteries. Nature 394:456–458

Gaberscek M, Dominko R, Jamnik J (2007) Is small particle size more important than carbon coating? An example study on $LiFePO_4$ cathodes. Electrochem Commun 9:2778–2783

Gao F, Tang ZY (2008) Kinetic behavior of $LiFePO_4$/C cathode material for lithium-ion batteries. Electrochim Acta 53:5071–5075

Gao J, Jiang CY, Ying JR, Wan CR (2006) Preparation and characterization of high-density spherical $Li_4Ti_5O_{12}$ anode material for lithium secondary batteries. J Power Sources 155:364–367

Ge H, Li N, Li DY, Dai CS, Wang DL (2008) Electrochemical characteristics of spinel $Li_4Ti_5O_{12}$ discharged to 0.01 V. Electrochem Commun 10:719–722

Huang Y, Qi Y, Jia D, Wang X, Guo Z, Cho WI (2011) Synthesis and electrochemical properties of spinel $Li_4Ti_5O_{12-x}Cl_x$ anode materials for lithium-ion batteries. J Solid State Electrochem. doi:10.1007/s10008-011-1611-5

Jiang CH, Hosono EJ, Zhou HS (2006) Nanomaterials for lithium ion batteries. Nanotoday 1:28–33

Jin B, Jin EM, Park KH, Gu HB (2008) Electrochemical properties of $LiFePO_4$-multiwalled carbon nanotubes composite cathode materials for lithium polymer battery. Electrochem Commun 10:1537–1540

Kim DK, Muralidharan P, Lee HW, Ruffo R, Yang Y, Chan CK, Peng HL, Huggins RA, Cui Y (2008) Spinel $LiMn_2O_4$ nanorods as lithium ion battery cathodes. Nano Lett 11:3948–3951

Liu H, Wang GX, Park JS, Wang JZ, Liu HK, Zhang C (2009) Electrochemical performance of α-Fe_2O_3 nanorods as anode material for lithium-ion cells. Electrochim Acta 54:1733–1736

Maier J (2007) Size effects on mass transport and storage in lithium batteries. J Power Sources 174:569–574

NuLi YN, Zeng R, Zhang P, Guo ZP, Liu HK (2008) Controlled synthesis of α-Fe_2O_3 nanostructures and their size-dependent electrochemical properties for lithium-ion batteries. J Power Sources 184:456–460

Qi YL, Huang YD, Jia DZ, Bao SJ, Guo ZP (2009) Preparation and characterization of novel spinel $Li_4Ti_5O_{12-x}Br_x$ anode materials. Electrochim Acta 54:4772–4776

Qiao H, Xiao LF, Zhang LZ (2008) Phosphatization: a promising approach to enhance the performance of mesoporous TiO_2 anode for lithium ion batteries. Electrochem Commun 10:616–620

Shen PZ, Jia DZ, Huang YD, Liu L, Guo ZP (2006) $LiMn_2O_4$ cathode materials synthesized by the cellulose–citric acid method for lithium ion batteries. J Power Sources 158:608–613

Wang YQ, Wang JL, Wang J, Nuli YN (2006) High-rate $LiFePO_4$ electrode material synthesized by a novel route from $FePO_4{\cdot}4H_2O$. Adv Funct Mater 16:2135–2140

Wang YG, Liu HM, Wang KX, EiJi H, Wang YR, Zhou HS (2009) Synthesis and electrochemical performance of nano-sized $Li_4Ti_5O_{12}$ with double surface modification of Ti(III) and carbon. J Mater Chem 19:6789–6795

Yi TF, Shu J, Zhu YR, Zhu XD, Zhu RS, Yue CB, Zhou AN, Zhu RS (2009) High-performance $Li_4Ti_{5-x}V_xO_{12}$ ($0 \le X \le 0.3$) as an anode material for secondary lithium-ion battery. Electrochim Acta 54:7464–7470

Yi TF, Shu J, Zhu YR, Zhu XD, Zhu RS, Zhou AN (2010) Advanced electrochemical performance of $Li_4Ti_{4.95}V_{0.05}O_{12}$ as a reversible anode material down to 0 V. J Power Sources 195:285–288

Yuan T, Cai R, Wang K, Ran R, Liu S, Shao ZP (2009a) Combustion synthesis of high-performance $Li_4Ti_5O_{12}$ for secondary Li-ion battery. Ceram Int 35:1757–1768

Yuan T, Wang K, Cai R, Ran R, Shao ZP (2009b) Cellulose-assisted combustion synthesis of $Li_4Ti_5O_{12}$ adopting anatase TiO_2 solid as raw material with high electrochemical performance. J Alloy Compd 477:665–672

Yuan T, Cai R, Gu P, Shao ZP (2010) Synthesis of lithium insertion material $Li_4Ti_5O_{12}$ from rutile TiO_2 via surface activation. J Power Sources 195:2883–2887